Hydrogen photosensitization, photochromism, and surface-enhanced infrared absorption in AgI thin films

A. I. Gavrilyuk
A.F. Ioffe Physical Technical Institute of Russian Academy of Sciences, 26 Polytekchnicheskaya Street, 194021 Sankt-Petersburg, Russia
(Received 23 June 2006; revised manuscript received 9 March 2007; published 9 May 2007)

Atomic photochemical hydrogen was produced by two methods: either employing a special hydrogen generator (a WO_3 thin film) or directly via a photochemical reaction on the surface of AgI films, with the atomic hydrogen being detached under the action of light from especially selected hydrogen-donor molecules previously adsorbed on the halide surface. The aim was to organize doping of the AgI film surface by atomic hydrogen, which yielded hydrogen sensitization simultaneous to illumination. Photochromism was achieved in the AgI evaporated films, which has been never observed before. Being an excellent reducing agent, the atomic hydrogen triggers formation of sensitization centers at the AgI surface, which provides, in turn, growth of nanosized silver clusters and colloids under the action of light. In fact, a composite material was created consisting of AgI, Ag, and hydrogen-donor molecules adsorbed on the AgI film surface and over the silver particles. The surface-enhanced infrared absorption (SEIRA) for the absorption bands attributed to vibrations of the hydrogen-donor molecules was observed in this composite, with the silver colloids of ~20 nm in diameter being formed in the AgI films under illumination, which are the best substrates to observe SEIRA. SEIRA, in turn, appears to be a very helpful method in the investigation of the hydrogen abstraction reaction yielding other evidences of the photoinitiated detachment of hydrogen atoms from the hydrogen-donor molecules. This paper will be of interest for many scientists in various branches of solid-state physics, materials physics, and nanoscience.

DOI: 10.1103/PhysRevB.75.195412 PACS number(s): 78.66.−w, 81.07.−b, 78.30.−j

I. INTRODUCTION

The physical and chemical properties of AgI have been extensively studied, since AgI is a material in electrolytes,[1] cloud condensation nuclei,[2,3] and photography.[4] Investigations of the photographical properties of the silver halide films and, especially, their predisposition toward defect formation under UV irradiation may supplement widely proceeding investigations of photographic emulsions (microcrystals of silver halides embedded in gelatin) and yield new important information concerning various aspects of the photographic process.

However, despite its tremendous significance, the photographical process is only a part of the wider subject, namely, formation of point and extended defects under the action of light,[5] which is of interest for many other topics, such as, e.g., formation of nanosized silver colloids and clusters[6–27] which can act as exceptionally active catalysts or photocatalysts in energy conversion, chemistry, and biology, as well as elements of photonic crystals or as substrates for surface-enhanced Raman scattering (SERS) and surface-enhanced IR absorption (SEIRA).[24–27]

Despite intensive investigations of preparation and properties of silver nanoparticles, there is a significant gap concerning the photolysis in the solid silver halides, which stimulates interest in the investigations of the defect formation in the silver halide films under the action of light.

However, the main point of the paper is the role of atomic hydrogen in the photolysis of the silver halide films. Being an excellent reducing agent, often a latent agent, and playing the role of a dopant or a catalyst, sometimes, combining both functions, atomic hydrogen triggers various processes on the solid surface. The employment of the photochemical hydrogen, detached from hydrogen-donor molecules via photochemical surface reactions, yields a new spirit in the study. The subject may be of interest for a wide circle of workers dealing with materials science, surface science, nanoscience, etc.

Photochromism in silver halides under illumination by photons with the energy exceeding the halide forbidden energy gap occurs due to photolysis in these materials. Photolytic silver atoms assemble in metallic colloids, which yields a new optical absorption band due to surface plasmons. This phenomenon was termed by Mott and Gurney[5] as the "the printout effect."

Evaporated AgI films hold the very special position concerning the photochromism: the printout effect under normal conditions was observed in evaporated AgCl thin films[28] and in evaporated $RbAg_4I_5$ thin films,[28–31] which have the structure very similar to that of AgI whereas the AgI thin films, evaporated onto unheated substrates, exhibit absolute insensitiveness to the action of light, either in air or under vacuum, even after very long exposures.

Low predisposition of AgI to photolysis compared with other silver halides was already discussed.[32,33] The first reason for that is the direct band gap in the electronic structure of AgI,[32] which results in a short lifetime of the photoexcited state before recombination of electrons and holes. Second, by first-principles molecular-orbital calculations, it was shown that AgI has lower predisposition toward silver cluster formation under the action of light as compared with other silver halides. In the presence of an interstitial Ag_i, the Ag_i–Ag bond is much weaker than the Ag–I bond at normal sites, whereas the formation of strong Ag_i–Ag bonds is essential for the agglomeration of silver atoms;[33] thus, the formation of a silver cluster meets difficulties in AgI. The cal-

culations were carried out for γ-AgI, although the authors claimed their validity also for β-AgI.[33]

On the other hand, the photolysis was achieved in polymorphous AgI single crystals consisting of β-AgI and γ-AgI,[34,35] as well as in amorphous thin films prepared by deposition from solutions[34] and in single-crystal films of AgI,[36] although the paper does not contain the information concerning the film structure. To understand the mechanism of the photolysis, one should carefully investigate the properties of AgI in connection with the structure and the method of preparation paying special attention to the difference in the surface morphology.

To achieve the printout effect in evaporated AgI thin films, an attempt was made to carry out hydrogen sensitization similar to the hydrogen hypersensitization of photographic emulsions provided by treatment in atmosphere of molecular hydrogen.

The chemical reaction of formation of hydrogen hypersensitization centers should be as follows:[4]

$$2\mathrm{AgI} + \mathrm{H}_2 \rightarrow \mathrm{Ag}_2 + 2\mathrm{H}^+ + 2\mathrm{I}^-. \quad (1)$$

Depending upon a surface grain site where they are formed, the reduction sensitization centers Ag_2 can either scavenge photogenerated holes or trap photogenerated electrons.[37] The possible reaction of a hydrogen reduction sensitization center, R center (Ag_2 at a neutral site of the grain surface), with a hole followed by production of two interstitial silver ions and a free electron[38] is

$$\mathrm{Ag}_2 + h^+ \rightarrow \mathrm{Ag}^+ + \mathrm{Ag} \rightarrow 2\mathrm{Ag}^+ + e^-, \quad (2)$$

where h^+ and e^- represent a positive hole and a free electron, respectively.

Recently, a new model was proposed manifesting that a reduction sensitization center P based on a silver dimer at positively charged kink site is not Ag_2 but merely Ag_3^+ at a negatively charged kink site of the grain surface, or to say more exactly, $Ag_3^{+1/2}$, since the charge of a kink site is one-half of one electronic charge.[39] Such P center then acts as an electron trapping center under illumination:[39]

$$\mathrm{Ag}_3^{+1/2} + e^- \rightarrow \mathrm{Ag}_3^{-1/2}. \quad (3)$$

Then, this center can combine a mobile interstitial Ag^+ forming a four-body cluster (latent image center):

$$\mathrm{Ag}_3^{-1/2} + \mathrm{Ag}^+ \rightarrow \mathrm{Ag}_4^{+1/2}. \quad (4)$$

Repetitions of the consecutive captures of electrons and positive silver ions yield a growth of the silver particle. So, two types of the hydrogen sensitization centers can be formed on the halide surface depending on the site where they are formed: R centers which are being destroyed under illumination scavenging photogenerated holes and generating Ag^+ interstitials and electrons and P centers which grow under illumination to silver particles.

The idea of this work was to carry out the hydrogen sensitization via the doping of the halide surface by hydrogen atoms detached from the adsorbed molecules simultaneously to illumination, which facilitates the photolysis due to formation of the sensitization centers Ag_2. Obviously, one may expect a higher sensitization effect in the case of the atomic hydrogen compared with H_2 [see Eq. (1)], since, in the latter case, no activation energy is required for dissociation of H_2 molecule.

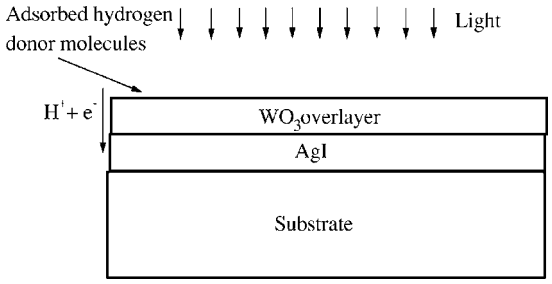

FIG. 1. The double-structure AgI-WO_3.

Meanwhile, the detached hydrogen atoms may act itself as an electron-hole pair donating electrons to a growing silver particle, which provides the conditions for further adherence of a silver interstitials Ag^+ [see Eqs. (3) and (4)]. First phototriggered hydrogen spillover was used for the hydrogen doping of the halide simultaneous to illumination.

II. HYDROGEN SENSITIZATION ACHIEVED VIA HYDROGEN SPILLOVER

A. The essence of the phototriggered hydrogen spillover

The hydrogen sensitization in the AgI films was carried out with the help of a double-layer structure consisting of consecutively evaporated AgI and WO_3 thin films[28] (Fig. 1) to provide the phototriggered hydrogen spillover.

WO_3 belongs to the family of "hydrogenphilics," loving hydrogen materials, capable of accommodating and transporting great amounts of hydrogen atoms. The interest to WO_3 was heated up by the pioneering work by Deb,[40] which initiated intensive investigations of electrochromism and photochromism[41] in this oxide. One can see recent reviews on the photochromism in transition-metal oxides in Refs. 42 and 43.

A WO_3 thin film can play the role of a catalyst in photochemical hydrogen abstraction reactions, if especially selected organic molecules (hydrogen donors) are adsorbed on the WO_3 film surface.[44–46] Hydrogen atoms were detached from the adsorbed molecules as the result of excitation of the WO_3 film surface by photons with the energy exceeding the oxide forbidden energy gap and transfer of surface excitation to the adsorbed molecules.[44–47] The WO_3 thin film played the role of a generator for hydrogen atoms in the double-layer structure. First, the photodetached hydrogen atoms were transferred from the donor molecules to the oxide surface as follows:

$$\mathrm{WO}_3(R\mathrm{H}_n)_{\mathrm{ads}} + h\nu \rightarrow \mathrm{H}_x\mathrm{WO}_3(R\mathrm{H}_{n-x})_{\mathrm{ads}}, \quad (5)$$

where $(R\mathrm{H}_n)_{\mathrm{ads}}$ is the adsorbed molecule (hydrogen donor) and H_xWO_3 the hydrogen tungsten bronzes.[41] It is well known that hydrogen atoms, being implanted into WO_3, donate electrons to the host turning into protons.[41] The amorphous WO_3 thin films have good electron and proton conductivity and a low value of the electron work

function,[43,48,49] providing transfer of the electrons and the protons between the WO_3 and the AgI films.[28] Migrating through interlayer grain boundaries of the WO_3 film, the electrons (e^-) and the protons (H^+) eventually reach the surface of the AgI film. Then, similar to the hydrogen hypersensitization [Eq. (1)], the surface reaction can occur producing the sensitization centers Ag_2 as follows:[31]

$$2AgI + 2H^+ + 2e^- \rightarrow Ag_2 + 2(H^+ + I^-). \quad (6)$$

The parentheses show that the guest protons are localized in the vicinity of iodine anions I^-. Canceling $2H^+$ in both sides of Eq. (6), it is possible to write

$$2AgI + 2e^- \rightarrow Ag_2 + 2I^-. \quad (7)$$

Equation (7) shows the essence of the hydrogen photosensitization: this is a redox process initiated in the host material by the guest electrons, whereas the guest protons play the role of charge compensators. On the other hand, microscopically, the photoinjection of electrons and protons into AgI may be considered as injection of movable defects, which, in turn, facilitates formation of point defects under illumination via collapse of electron excitation in the vicinity of injected impurity atoms.[50,51] The injection of hydrogen atoms facilitates also the agglomeration of silver atoms; the protons, being localized in the vicinity of I^- anions, weaken the Ag–I bonds. There are two types of excitation of the halide surface: short-lifetime excitation by light and indefinitely long-lifetime "excitation" by the hydrogen atoms (the electrons and the protons), with both the point defect formation and the agglomeration of silver atoms being facilitated. The combined action of both excitations makes it possible to overcome the inherent drawbacks of AgI concerning the predisposition to the photolysis. The hydrogen sensitization triggers the further growth of silver particles [see Eqs. (2)–(4)].

The double-layer structure realizes the idea of two-stage catalysis: first, the oxide surface catalyzes hydrogen production under the action of light, and then the photochemical hydrogen atoms act as catalysts in the photolysis of the halide.

B. The double-layer structure preparation and characterization

The AgI films were prepared by thermal evaporation of AgI 99.99% purity powder onto unheated KBr or quartz substrates. Temperature of an evaporation boat was maintained at 600 °C. The preparation method, characterization, and the optical properties of the films were described elsewhere,[52–54] with the films being polycrystalline and consisting, predominantly, of β-AgI (wurtzite) with small amount of γ-AgI (zinc blende).[52–54] Film thickness was determined by measuring the distance between two neighboring lowest-energy interference minima or maxima in the optical-density spectra, with the refractive index being taken $n=2.05$.[55]

The optical-density spectrum at room temperature has a relatively narrow exciton band at $E=2.92$ eV ($\lambda=425$ nm), which was reported before[52–54] (Fig. 2, curve 1). The film grain size ranged within 0.5–1 μm.

The WO_3 film was deposited by evaporation of the 99.99% purity powder from a tungsten boat heated up to 1300–1400 °C.[28,48,49] The substrates with the deposited AgI films were not especially heated; their temperature reaches 40–50 °C during the evaporation due to heat radiation from the evaporation boat. The WO_3 films were prepared thin enough to provide illumination of the AgI surface simultaneously to the hydrogen spillover. Reference samples, "pure" WO_3 film deposited onto transparent substrates, were also prepared in one technological run together with the double-layer structures; the film thickness is determined by the same method as for the AgI films and the refractive index is taken to be $n=2.2$.[40]

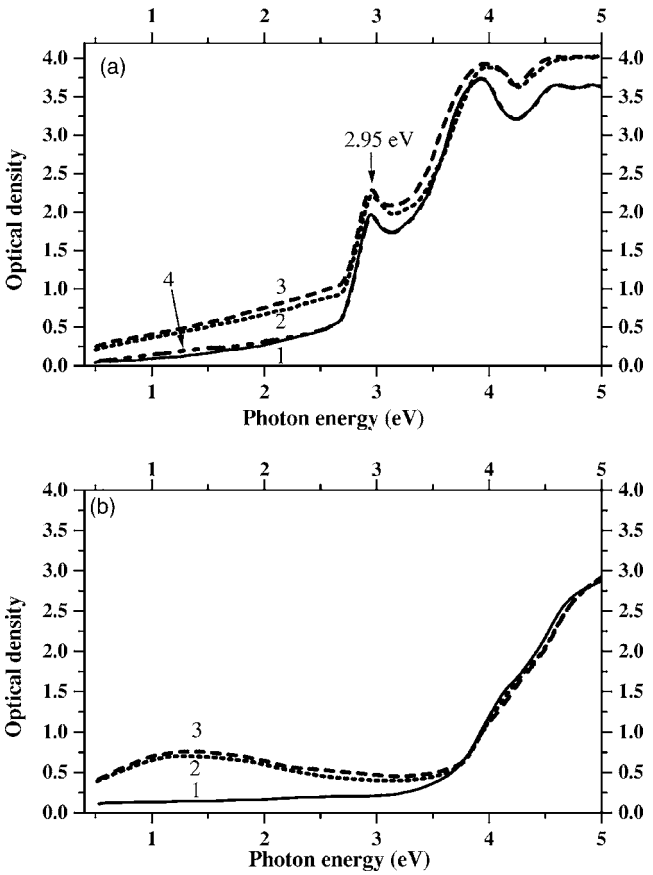

FIG. 2. Optical-density spectra before and after illumination in methanol vapor: (a) for the double-layer structure AgI-WO_3 and (b) for the WO_3 reference film prepared in one evaporation run together with the double-layer structure. (1) Before illumination; after illumination in methanol vapor for (illumination time t), (2) $t=1$ h, (3) $t=3$ hours; and (4) after illumination of the reference heterostructure under a vacuum of 10^{-2} mbar for $t=1$ h. Film thickness d: for AgI film, $d=0.4$ μm; for WO_3 film, $d=0.2$ μm.

C. Experimental details

Methanol (CH_3OH) was used as a source of hydrogen atoms.[28] Illumination was carried out in a sealed cell, previously pumped to a vacuum of 10^{-2} mbar, in methanol vapor at 30 mbar pressures. The optical-density spectra were measured with the help of a double-beam spectrophotometer SF-8 (LOMO PLC).

The AgI thin films were illuminated from a 250 W power mercury lamp with a quartz envelope whose spectrum of

irradiation contains a series of bands in the UV range of relative intensity stated in the brackets at $E=3.4$ eV (100%), $E=3.96$ eV (68%), $E=4.1$ eV (31.3%), $E=4.175$ eV (14.2%), $E=4.43$ eV (10.3%), $E=4.68$ eV (23.4%), $E=4.88$ eV (26.1%), and $E=5$ eV (10.5%). The irradiation spectrum also contains three bands in the visible at $E=2.14$ eV (70.4%), $E=2.27$ eV (72%), and $E=2.85$ eV (62.4%), and one band exactly on the border between the visible and UV ranges at $E=3.05$ eV (35.9%). For the sake of acceleration of the experiments, the full lamp output was used, with the samples being illuminated through a water filter to get rid of IR components of the radiation. The special measures were undertaken to prevent heating of the samples, with the highest temperature not exceeding 45 °C during illumination. Irradiation of nearly all bands was totally absorbed within the WO_3 film providing detachment of hydrogen atoms from the adsorbed molecules, except for the irradiation of two bands at $E=3.05$ eV and $E=3.4$ eV, which penetrated through the WO_3 film illuminating the AgI surface and generating electron-hole pairs in the halide, which can be seen from Fig. 2(b) showing the optical-density spectrum for the WO_3 reference film before illumination (curve 1).

D. Results and discussion

The optical-density spectra before (curve 1) and after illumination of the AgI-WO_3 structure are shown in Fig. 2(a) (curves 2 and 3): a wide band arises covering the whole visible range and spreading into the near-IR range. Figure 2(b) shows the optical-density spectra for the WO_3 reference film illuminated under the same conditions.

The changes in the spectra [Fig. 2(a)] cannot be explained by the photoinjection of hydrogen only into the WO_3 film: in the latter case, a wide absorption band would arise peaking at $E=1.25$ eV ($\lambda=1000$ nm) [see Fig. 2(b) (curves 2 and 3)], which has nothing in common to that presented in Fig. 2(a) (curves 2, 3).

One can realize that the optical-density spectra in Fig. 2(a) may be interpreted as a superposition of the absorption bands arising in the WO_3 film (Fig. 2(b)) and an absorption band arising in the AgI films; a new band peaks in the range $E\sim 2-3$ eV, which implies that the printout effect in the evaporated AgI films can be achieved if the halide surface is doped with hydrogen atoms simultaneous to illumination. However, the photolysis is interrupted at an early stage. The most probable reason seems to be a continuous blockade of the oxide interlayer grain boundaries by the photolytic silver. The grain boundaries form specific channels for migration of the detached hydrogen atoms. If these channels are being continuously blockaded during the photolysis, the process eventually stops.

This hypothesis is confirmed by the fact that the heterostructures consisting of the silver or cuprous halide films and the WO_3 film lose their photochromic sensitivity to essentially zero by storage under normal conditions either under vacuum or in air for several days after preparation, whereas the reference WO_3 film, prepared by evaporation onto any dielectric substrate in one run with the heterostructures, does not. The total loss of the sensitivity for the oxide film indicates that it loses not only at the interface with the halide but also at the film surface. Thus, there is a slow (ionic) process proceeding over the whole film thickness, and it could be tentatively suggested that it is connected with the diffusion of silver or copper ions, since it is well known that these ions are mobile in the halides.[4,5] It is important to stress that the experiments were always carried out with in as-prepared samples; the illumination of the heterostructure, either in vacuum or in air, was carried out without methanol vapor, yielding only insignificant changes in the optical-density spectra [Fig. 2(a), curve 4]. This small effect is attributed to "wild" photochromism in the amorphous WO_3 films arising due to hydrogen atoms, detached from hydrogen-containing molecules (water and organics), uncontrollably adsorbed on the oxide surface during preparation, or from ambience. Obviously, this effect is very small compared with the "cultivated" photochromism when the especially selected hydrogen-donor molecules (of methanol) are adsorbed in great quantities on the oxide surface.[44–47] Curve 4 in Fig. 2(a) presents the maximum effect which can be achieved under illumination under vacuum; the process is interrupted after some exposure due to exhaustion of occasional hydrogen source.

The printout effect achieved first in the AgI films[28] was not very bright, and additional experiments were required to clarify what is going on. It makes sense to return to the discussion concerning the data presented in Fig. 2 after the description of other results. Despite all these drawbacks, the method of hydrogen spillover was a very important step in the investigations of the photochromism in AgI films, since it was the very first achievement of the effect via the hydrogen sensitization,[28] which, in turn, stimulated the search for new methods of deeper photolysis in this material.

III. DIRECT PHOTOINJECTION OF HYDROGEN IN AgI

A. The essence of direct photoinjection of hydrogen in AgI

To achieve deep photolysis in the AgI thin films, one should find a method to carry out the direct photoinjection of hydrogen into the halide, for which an appropriate molecule (hydrogen donor) should be found. The ability of the silver complexes in the donor-acceptor bonding with nitrogen-containing molecules was the basis for the search for the possible hydrogen donor. The idea of the direct photoinjection of hydrogen was similar to that achieved in the transition-metal oxide films (WO_3, MoO_3, and V_2O_5), where hydrogen atoms were detached from adsorbed organic molecules bonded to the oxide surface via donor-acceptor and hydrogen bonds. The hydrogen atoms were transferred to the oxide surface as the result of the photostimulated reaction of hydrogen transfer.[44–47]

The objective was achieved by the use of diethylamine (DEA) $[(C_2H_5)_2NH]$ as the hydrogen donor. The donor-acceptor bonding between a silver surface ion Ag^+ of AgI and DEA can arise with the help of a lone electron pair of nitrogen atom of the DEA molecule, which yields polarization of the N–H bond within the molecule. It is well known

that ammonialike compounds form complex cations with silver ions;[4] perturbation of this bond weakens it, whereas the polarization facilitates the hydrogen bonding between H atoms of DEA and surface anions I^-. Thus, at least some of the adsorption complexes are able to detach hydrogen atoms under the action of light if the surface is illuminated by photons with the energy exceeding the forbidden energy gap of AgI, via the reaction of proton coupled electron transfer:[47,56] first, an electron of a lone pair of a nitrogen atom of the adsorbed organic molecule scavenges a photogenerated hole in the valence band of AgI (electron transfer), and then the hydrogen-bonded proton is transferred between the adsorbed molecule and the surface I^- of AgI. Then, the hydrogen sensitization *R* and *P* centers arise, and the photolysis proceeds further as described above [see Eqs. (2)–(4)].

B. Experimental details

Illumination of the AgI films in DEA vapor by light quanta from each of the energy bands in the UV range discriminated from the full lamp output with the help of interference filters yields the photochromism in the AgI films. As in previous case, for the sake of acceleration of the experiments, the full lamp output was used illuminating the samples through a water filter in a sealed, previously evacuated to 10^{-2} mbar vacuum cell in DEA vapor at a 10 mbar pressure.

C. Results and discussion

The successful finding of the appropriate hydrogen donor yielded the drastic printout effect in the AgI films, which is illustrated by Figs. 3 and 4, where the optical-density spectra before and after several exposures of the AgI films in DEA vapor are presented. Two films of different thicknesses were employed to demonstrate various aspects of the photochromism. For the sake of clear presentation of all details, Figs. 3 and 4 are divided in two parts [(a) and (b)].

At the early stage of the photolysis [Fig. 3(a), curves 2 and 3, or Fig. 4(a), curves 2–4], a new broad optical absorption band arises peaking at the border between the visible and UV ranges.

At longer exposures, the optical-density spectra are changed drastically [Fig. 3(b), curves 4–6, and Fig. 4(b), curves 5–7]. The exciton band at $E=2.95$ eV ($\lambda=420$ nm) disappears, making it clear that this band had hidden the other optical band peaked at $E=2.9$ eV ($\lambda=425$ nm) whose intensity continuously grows with exposure. Going back to Fig. 2(a), one gets an additional evidence to consider the optical absorption band presented in curves 2 and 3 as a superposition of the bands peaked at $E=2.9$ eV ($\lambda=425$ nm) and $E=1.25$ eV ($\lambda=1000$ nm) arising in the AgI films and the WO_3 films, correspondingly, [Fig. 2(a)] due to injection of hydrogen atoms.

The appearance of very broad bands peaked at $E=2.1-2.9$ eV is very common in silver halides. The band at $E=2.9$ eV ($\lambda=0.425$ nm) is not bleached under illumination by the visible light, as for *F* centers. It bleaches out after long-time (for several months) storage at room temperature

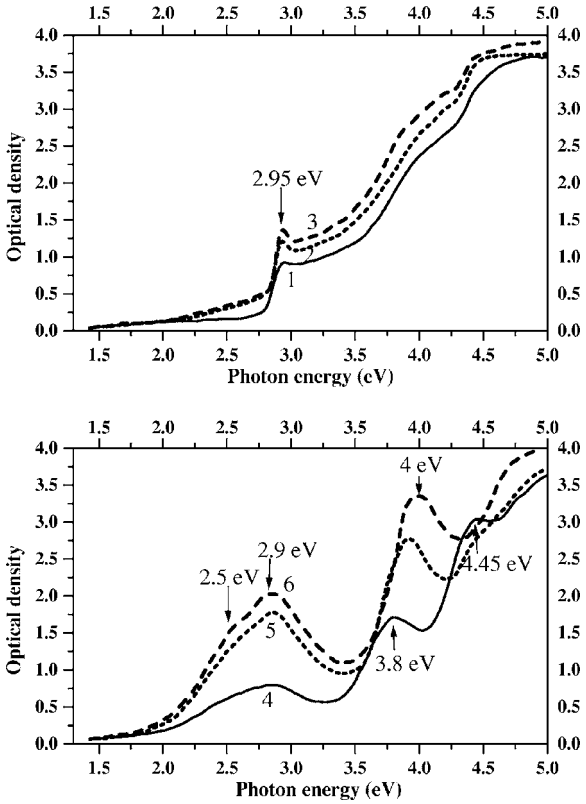

FIG. 3. Optical-density spectra for 0.3 μm thick AgI film before and after illumination in DEA [vapor: (1) before illumination, (2) after illumination for (illumination time *t*), (2) $t=10$ min, (3) $t=30$ min, (4) $t=1$ h, (5) $t=2$ h, and (6) $t=4$ h.

in oxygen-containing ambience, being stable under the same conditions under vacuum. All these features give the possibility to assign this band to the absorption by metallic colloids of the photolytic silver due to surface plasmons.[6–27] At the same time, it is possible to see that the optical absorption band attributed to the surface plasmons in the silver particles is not elementary: the second peak revealed as a shoulder at $E=2.5$ eV is observed in Figs. 3(b) and 4(b).

Theoretical studies and experimental works have shown that dipolar absorption is dominant for particles <20 nm, whereas in larger particles, dipolar scattering and quadrupolar absorption play significant roles leading to noticeable broadening of the absorption band. The position and the number of peaks in the absorption spectra reveal also the morphology of the particles, whereas the dielectric constant of the solvent plays an important role. For example, spherical particles show only one band peaked at about $E=3.1$ eV (400 nm), whereas for ellipsoid particles, two peaks appear in the absorption band.[16] In the literature, there are several explanations for the appearance of the broad extinction band at longer wavelength. Some authors have attributed it to the presence of a second distribution of larger, elongated, or polydispersed particles.[17] Others have suggested that it arises from light extinction due to higher-order surface plasmon modes resulting from interactions of nanoparticles;[18,19] its origin is postulated by assuming the presence of aggregates of primary particles interacting collectively with the incident light as a large silver particle.[20–22] The aggregation of par-

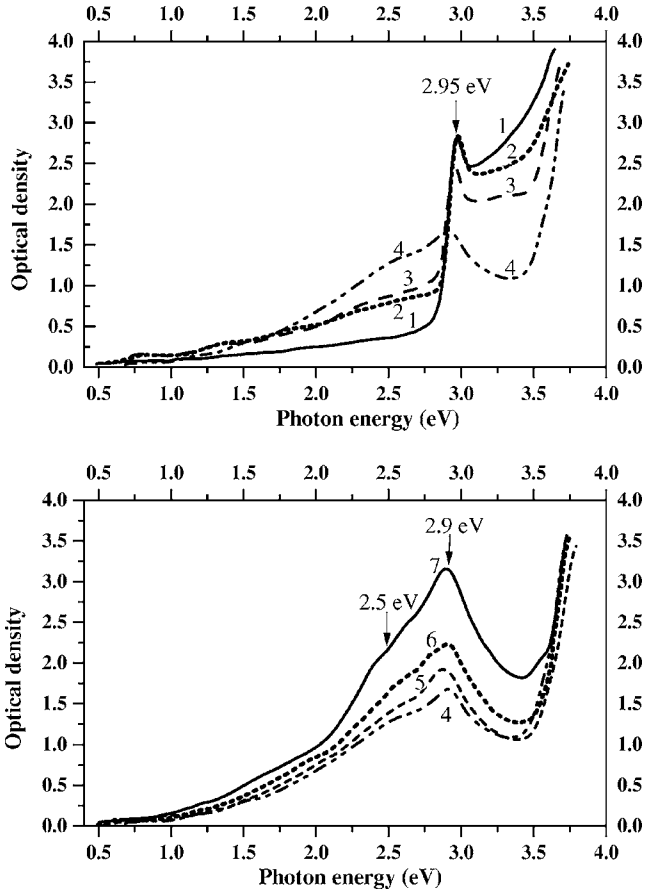

FIG. 4. Optical-density spectra for 0.6 μm thick AgI film before and after illumination in DEA vapor: (1) before illumination and after illumination for (illumination time t) (2) $t=3$ min, (3) $t=15$ min, (4) $t=1$ h, (5) $t=2$ h, (6) $t=4$ h, and (7) $t=9$ h.

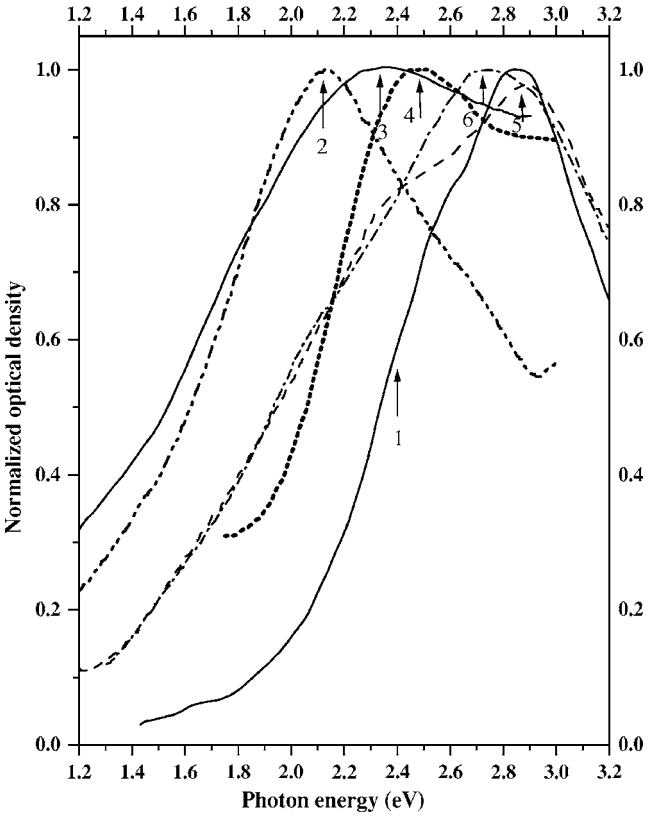

FIG. 5. Normalized absorption band D/D_{max} arising in the silver halide films under illumination (1) for the AgI film illuminated in DEA vapor, (2) for the AgCl film illuminated under vacuum (Ref. 44), (3) for the $RbAg_4I_5$ film illuminated under vacuum (Ref. 31), and [(4)–(6)] for the $RbAg_4I_5$ film illuminated in DEA vapor (Ref. 31) for (illumination time t) (4) $t=5$ min, (5) $t=1$ h, and (6) $t=8$ h.

ticles takes place when particles of different sizes bump into one another. A tendency for metal ions to dissolve from the surface of smaller Au particles and precipitate on the surface of larger ones has been shown.[23] Therefore, to reduce the possibility of bumps between particles and to prevent the aggregation of particles, polymeric stabilizer and organic solvent are used.

The presence of two bands in the optical-density spectra attributed to the surface plasmons, one peaking at $E=2.9$ eV and the other revealed as a shoulder at about $E=2.5$ eV [Figs. 3(b) and 4(b)], indicates that two types of metallic silver colloids are formed under illumination in DEA vapor: small-sized sphere shaped and large sized of more complicated morphology. The relatively narrow band peaked at $E=2.9$ eV is attributed to the small-sized colloids, whereas the band at $E=2.5$ eV to the large-sized ones.

For the sake of completeness of the consideration, the normalized optical-density spectra calculated as a ratio of the optical density D to the maximum optical density D_{max} in the band are presented in the range 1.2–3.1 eV (Fig. 5), which demonstrate the peculiarities of the printout effect in various silver halide films. The calculations were made on the basis of the data presented in this paper (AgI) and previously published papers [Ref. 31 ($RbAg_4I_5$) and Ref. 44 (AgCl)]. The wide consideration is important and visual for further generalizations, as well as for determination of the specific features of the AgI films in comparison with other halide films regarding the properties of the photolytic silver particles precipitated in these materials, as well as the run of the photolysis (Fig. 5).

First, the normalized optical-density spectra for the $RbAg_4I_5$ thin films, close "relatives" of the AgI films, are presented, which have structure and properties similar to the latter. The printout effect in these films observed under vacuum can be drastically enhanced in DEA vapor,[31] with the condition of illumination as mentioned before. The normalized optical-density spectra for the $RbAg_4I_5$ are calculated from the data presented in Ref. 31. As it can be easily seen from comparison of curve 3 and curves 4–6 in Fig. 5, there is a significant difference in the optical-density spectra in the position and width of the bands attributed to the silver colloids, depending on whether illumination is carried under vacuum or in DEA vapor.

Similar spectra calculated from the data in Ref. 44 are presented, which illustrate the printout effect in AgCl films illuminated under vacuum (Fig. 5, curve 2).

For the AgI (curve 1), the AgCl (curve 2), and the $RbAg_4I_5$ (curve 3) films illuminated under vacuum, it is sufficient to present only one typical normalized optical-density

D/D_{max} spectrum, since the character of the absorption slightly changes during the illumination. Obviously, for the AgI films, only the data presented in Fig. 3(b) can be used for the calculation of the normalized absorption band, since at the early stage of the process [Fig. 3(a)], the presence of the exciton band peaked at $E=2.95$ eV makes it senseless.

The different case is observed in the $RbAg_4I_5$ films illuminated in DEA vapor: the position of the normalized band changes significantly with exposure. For this reason, three curves D/D_{max}, calculated from the spectra of the $RbAg_4I_5$ films after several exposures (Fig. 2 of Ref. 31), are presented in Fig. 5 (curves 4–6).

It is important to emphasize that the changes in the optical-density spectra are influenced not only by the appearance of the photolytic silver but also by fracture of grains during the process. The splitting of the grains along the crystallographic planes and formation of the internal cracks where new silver specks can be precipitated are common in silver halides.[5] The fracture of AgI single crystals, containing β-AgI and γ-AgI, under the action of light was observed before.[34,35] The authors claimed that the reasons are the consecutive growth of γ-AgI filaments within β-AgI and the formation of dipole complexes together with silver specks at the border between β-AgI and γ-AgI, which leads first to the division into layers and then to the fracture of the crystals.[34,35]

The fracture of grains leads to a decrease of light scattering in the AgI films, which is better revealed in thick samples: in the spectra for the thicker AgI films, the substantial decrease of the optical density is observed in the range 3.0–3.6 eV [Fig. 4(a)] together with the increase of the amplitude of the interference fringes in the range 0.5–1.5 eV [Fig. 4(a), curves 3 and 4]. The decrease of the light scattering during the photolysis can also be easily observed by visual examination of various subjects through the AgI film deposited onto transparent substrates.

The absorption band arising in the AgI films (Fig. 5, curve 1) peaks at $E=2.9$ eV. This relatively narrow band may be attributed to spherical silver particles of size <20 nm.[16] The other peak can be observed as a shoulder peaked at $E=2.5$ eV, indicating the presence of a definite share of large-sized colloids.

A relatively narrow band peaked at $E=2.2$ eV (Fig. 5, curve 2) arises in the AgCl films under illumination under vacuum, which may be attributed to the formation of large elongated colloids, which is also confirmed by the appearance of the second band peaked at $E=3.4$ eV. The appearance of two bands is typical for AgCl suspensions.[6] It is well known that AgCl has an enormous plasticity close to that of metals, which facilitates bumping of colloids and formation of large-sized particles.

The $RbAg_4I_5$ films exhibit the most interesting behavior, demonstrating the great difference in the spectra, which depends upon whether the films are illuminated under vacuum or in DEA vapor. When illumination is carried out under vacuum, one broad band arises peaking at $E=2.4$ eV; the position of the band maximum slightly shifts to lower energies with exposure (Fig. 5, curve 3).

A different case is observed in the $RbAg_4I_5$ films when illumination is carried out in DEA vapor. At the initial stage of the process, only one band arises peaking at $E=2.5$ eV (Fig. 5, curve 4). Although this band is narrower and slightly shifted to higher energies, it resembles that arising in these films under illumination under vacuum (Fig. 5, curve 3). At longer exposures, the appearance of two bands is observed, one peaking at $E=2.5$ eV and the other at $E=2.9$ eV (Fig. 5, curve 5). This case is very close to that observed in the AgI films. At longer exposures, merging of the both bands can be observed due to the shift of the band peaked at $E=2.9$ eV to lower energy, which indicates some enhancement in size for the small-sized colloids (Fig. 5, curve 6).

Thus, two kinds of the silver colloids, depending upon the properties of the halide and conditions of illumination, can arise: small-sized ($\sim$20 nm in size) close to sphere-shaped particles and large-sized polydispersed particles. The adsorption of DEA molecules over arising silver particles prevents there bumping, which, in turn, is reflected in the absorption spectra. The shift of the absorption band maximum to higher energies in the $RbAg_4I_5$ films illuminated in DEA vapor (Fig. 5, curve 4 and 5) is delayed at the beginning of the illumination.

Comparing the data presented in Fig. 5, it is possible to conclude that the smallest particles amongst the silver halides are formed in the AgI films, which is important for further discussions.

One can easily understand that the AgCl films are less than the other films inclined to the grain fracture, since they have the highest plasticity; plastic flow helps the growth of the large-sized photolytic silver particles. For this reason, the photolysis is easily achieved in these films without special hydrogen sensitization; not numerous nuclei easily grow in the large-sized particles.

The AgI films have much lower plasticity as compared with that for the AgCl films. The photolysis goes hard in the AgI films being achieved only via the hydrogen sensitization. Numerous hydrogen sensitization centers facilitate, in turn, formation of numerous growing silver nuclei. The mechanical stresses within the film AgI are enhanced with the growth of silver particles. When the stresses reach a critical value, the film grains are fractured yielding an enhancement of the film specific surface area, as well as size of pores, and interlayer grain boundaries, which, in turn, facilitates the access of DEA molecules to the halide surface and promotes further growth of the silver particles. On the other hand, the fracture of grains can lead to appearance of small-sized AgI fragments which can completely turn into silver particles during further photolysis. The grain fracture in the AgI films starts together with the beginning of the illumination, which can be easily seen from Fig. 4(a); the amplitude of the interference fringes increases together with the decrease of the absorption in the range 3.1–3.6 eV.

The $RbAg_4I_5$ films possess an intermediate position between two halides mentioned. They exhibit the photochromism under vacuum[31] without special hydrogen sensitization, which yields formation of the large-sized particles, similar to those arising in the AgCl.

At the initial stage of the illumination in DEA vapor (Fig. 5, curve 4), the $RbAg_4I_5$ films also reveal the tendency to the formation of the large-sized particles similar to the case of illumination under vacuum; then, after some exposure, the

number of the hydrogen sensitization centers is enhanced, initiating the growth of many silver particles which, in turn, yield the enhancement of the mechanical stresses within the film eventually leading to the grain fracture. The formation of the small-sized fragments and the access of DEA molecules to the surface of the arising silver particles are facilitated, which makes it possible to conserve the small-sized colloids. One can see the significant changes in the absorption spectra occurring due to the formation of the small-sized silver particles (Fig. 5, curves 5 and 6); the second optical band appears peaking at $E=2.9$ eV. Obviously, there is a time difference between the beginning of illumination and the beginning of the grain fracture: time is needed for the adsorption of the organic molecules penetrating into the grain boundaries and formation of numerous growing silver nuclei which eventually cause the critical mechanical stresses yielding the grain fracture.

Thus, two regimes of photolysis can be carried out in the $RbAg_4I_5$ films: either slow (under vacuum) or rapid (in DEA vapor). The rapid process is accompanied by the fracture of grains, whereas the slow is not. This yields the significant difference in the morphology of the arising silver particles, which is reflected, in turn, in the optical spectra. The case of the $RbAg_4I_5$ films is very important since it bridges very different cases of the AgI and the AgCl films.

Thus, the creation of the silver nuclei due to the intensive hydrogen photosensitization, and their growth, yielding the fracture of grains, makes it possible to conserve the small-sized spherical particles within the films preventing their bumping. It may be assumed that the disappearance of the exciton bands peaking at $E=2.95$ eV in the AgI films and at $E=3.35$ eV in the $RbAg_4I_5$ films[31] is attributed to the fracture of grains during the direct hydrogen sensitization, which yields a great degree of disorder.

After the disappearance of the exciton band, two new bands appear in UV range at $E=3.8$ eV ($\lambda=325$ nm) and $E=4.45$ eV ($\lambda=280$ nm), which can be observed in the thinner AgI films (Fig. 3), similar to those peaking at $E=4$ eV ($\lambda=310$ nm) and $E=4.3$ eV ($\lambda=290$ nm) in the $RbAg_4I_5$ films illuminated in DEA vapor.[31] The band at $E=3.8$ eV ($\lambda=325$ nm) is continuously shifting to higher energies up to $E=4.0$ eV ($\lambda=310$ nm), whereas the band at $E=4.45$ eV ($\lambda=280$ nm), arising first [Fig. 3(b), curve 4], disappears after longer exposures [Fig. 3(b), curves 5 and 6].

To identify these bands, one must first consider whether the new absorption bands in the UV range may be attributed to DEA molecules adsorbing on the halide surface during illumination. It is known[57] that the whole UV band can be conventionally divided into two parts, the energy $E=6.53$ eV ($\lambda=190$ nm) being a border. Intensive $\sigma\rightarrow\sigma^*$ optical transitions occur only at $E>6.53$ eV, whereas only much less intensive $n\rightarrow\pi^*$, $n\rightarrow\sigma^*$, $\pi\rightarrow\pi^*$, and $\pi\rightarrow\sigma^*$ transitions can be observed at $E<6.53$ eV. Since in our experiments the optical-density spectra were measured up to $E=4.5$ eV, the possibility of low-intensive optical transitions must only be considered. DEA molecule does not contain unsaturated bonds but contains a nitrogen atom with a lone electron pair in a nonbonding orbital; thus, only the possibilities of the $n\rightarrow\pi^*$ and $n\rightarrow\sigma^*$ transitions are to be taken into account. For example, a relative to DEA CH_3NH_2 molecule absorbs at $E=5.77$ eV ($\lambda=215$ nm) with an apparent molar extinction coefficient $\varepsilon_a=600$ l/mol cm.[57] Despite the fact that this band is out of the measured range, one can assume that due to adsorption, it might be shifted to the energies $E<4.5$ eV. A rough estimation can be made concerning the possible optical densities achieved due to those hypothetical electron transitions using the formula[57]

$$D=\varepsilon_a dc, \tag{8}$$

where D is the optical density, d the film thickness (in centimeters), and c the concentration of the adsorbed DEA molecules in (mol/l). The molecular weight of DEA is 73 g/mol, and the density is 0.7 g/cm^3. The adsorbed DEA molecules can fill $\sim$0.01–0.05 of the volume within the polycrystalline AgI film. It means that c is $\sim$0.1–0.05 mol/l. Then for the 0.3 μm thick film (Fig. 3), we get $D\approx 2\times 10^{-3}-10^{-2}$. However, Fig. 3(b) shows that the photoinduced optical density reaches the values of 1–2 for the band peaked at $E=3.8-4$ eV. Thus, one can state it with the following great margins: the new optical bands cannot be attributed to the optical transitions in adsorbed DEA molecules. It should be noted that the intensity of the band peaked at $E=3.8-4$ eV grows continuously with the intensity of the band attributed to the silver colloids [Fig. 3(b)], which implies that all bands arise due to the same reason. Similar behavior is exhibited by the bands at $E=4$ eV and $E=4.35$ eV in the $RbAg_4I_5$ films (Fig. 6).[31]

The absorption bands of energies >3 eV ($\lambda=400$ nm) are usually assigned to silver clusters Ag_n consisting of several atoms.[6,9,58] The band peaked at $E=4.45$ eV ($\lambda=280$ nm) was often observed in silver compounds and may be assigned to charged silver particles with the configuration Ag_4^{2+}.[6,9,58] The band at $E=3.8-4.0$ eV ($\lambda=310-325$ nm) can be merely assigned to neutral silver particles, possibly Ag_6.[58] The silver particles Ag_4^{2+} and Ag_6 belong to the family of the so-called magic clusters, which are relatively stable due their electronic and space structures.[58] Further investigations with the use of Raman and ^{109}Ag NMR spectra might be useful for specifying this tentative suggestion.

The disappearance of the band at $E=4.45$ eV ($\lambda=280$ nm) at long exposures occurs due to the bumping of the Ag_4^{2+} particles. The corresponding band at $E=4.3$ eV in the $RbAg_4I_5$ films does not disappear even after long exposures; compare Fig. 3(b) and Fig. 2 of Ref. 31. The shift of the band at $E=3.8$ eV ($\lambda=325$ nm) to $E=4.0$ eV ($\lambda=310$ nm) may occur due to the changes in the solvate shell of the clusters during illumination. On the other hand, the band attributed to the Ag_6 cluster in the $RbAg_4I_5$ films appears at $E=4$ eV and is not shifted during the illumination.[31] The difference in the position of the bands, their width, and behavior under illumination can be attributed to different solvate shells of the arising clusters in different materials. Comparing Fig. 3 and Fig. 2 in Ref. 31, one can easily find the significant difference in the width of the bands attributed to the silver clusters in the AgI and the $RbAg_4I_5$ films. The bands are much broader in the AgI films as compared with those in the $RbAg_4I_5$ films, which indicates higher degree of

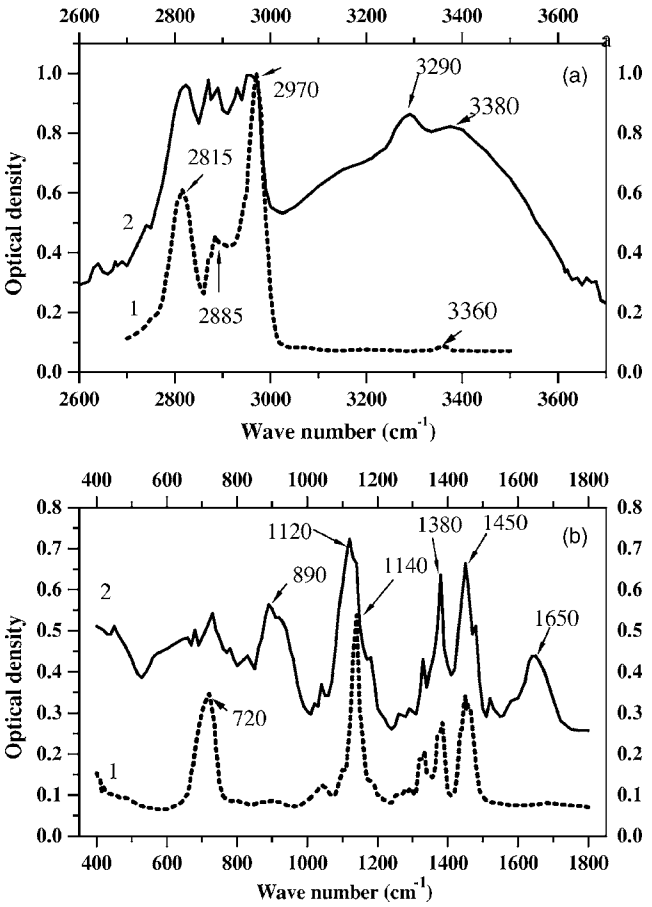

FIG. 6. Optical-density spectra for DEA molecules (1) in vapor (short-dotted line) (2) in liquid (solid line).

disorder occurring in the AgI films due to poor mechanical characteristics which determine higher inclination to the fracture of grains. The high degree of disorder, in turn, predetermines inclination to form the small-sized silver colloids, which is a significant feature for the AgI films. The ability to obtain and stabilize the nanosized silver clusters by the method presented is of special interest due to their specific chemical and catalytic properties.

It should be added that changes in the optical-density spectra were likely observed in the heterostructures consisting of a AgI thin film and a film of a $3d$ or $4f$ rare metal sputtered or evaporated onto the halide film surface.[53,54] After deposition of the metal films onto the AgI film, new absorption bands appeared in the optical-density spectra: one wide band peaked at ~2.5 eV and one or two narrower bands peaked in the range 3.4–3.7 eV. The authors assigned the latter bands to the excitons of the new phase.[53,54] However, the dark redox process in the AgI film initiated by deposition of the metal films on the halide surface can also yield decomposition of the AgI films, which causes the appearance of the silver colloids and the magic clusters.

IV. SURFACE-ENHANCED INFRARED ABSORPTION FOR HYDROGEN-DONOR MOLECULE

It has been shown that hydrogen photosensitization makes it possible to achieve the printout effect in the evaporated AgI films; the sensitization centers being formed promote photolysis of the halide and the appearance of the silver colloids and the magic clusters. The metal silver colloids are responsible for the changes of the optical properties in the visible, UV, and near-IR ranges, whereas the additional absorption bands arise in UV range due to the magic clusters. On the other hand, one can easily suspect that the necessary requirements might be fulfilled for observing surface-enhanced infrared absorption (SEIRA) and surface-enhanced Raman scattering (SERS) in the presented experiments: the silver nanosized particles are formed in atmosphere organic molecules adsorbing on their surface. The effect of surface enhancement due to plasmon excitations is well known for Raman spectroscopy.[59–62] The present study will be dealing with less common but similar effect which enhances infrared signals, i.e., SEIRA.

An incident IR light polarizes a metal particle which is much smaller than the wavelength; the dipole moment P being induced[63] takes the form

$$P = \alpha V E_i, \tag{9}$$

where α is the polarization susceptibility, V the volume of a particle, and E_i the electric field of the incident light. The dipole, in turn, induces a local electric field E_{loc} around the particle with the amplitude of the field[63] as follows:

$$E_{\mathrm{loc}} = 2P/d^3, \tag{10}$$

where d is a distance from the center of the particle. The local electric field is much stronger than the field of an incident light, which leads to an enhancement of the bands in the spectra of adsorbed molecules in the vicinity of the metal particle. This enhancement rapidly decreases with increasing distance from the particle surface.

The infrared adsorption A may be given as[64]

$$A \propto (\delta\mu/\delta Q)^2 E_{\mathrm{loc}}^2 \cos^2\theta, \tag{11}$$

where $\delta\mu/\delta Q$ is the derivative of the dipole moment with respect to a normal coordinate Q, E_{loc} the electric field exiting the molecule, and Q the angle between $\delta\mu/\delta Q$ and E_{loc}. The polarization susceptibility of the metal particles is modulated by the adsorbed molecules; the modulation is larger at frequencies of the inner-molecular vibrations than at other frequencies. This means that the absorbance of the metal particles will be changed at the molecular vibration frequencies. It is obvious that our system may be assumed as a continuous film composite consisting of Ag particles, adsorbed DEA molecules, and the host medium (AgI). For such type of the systems, the calculations of the reflectivity and absorbance were performed using the Fresnel equation.[64] The effective dielectric function of the composite film was connected to polarization susceptibility of metal particles by effective-medium approximation. The dielectric function was calculated using the Maxwell-Garnet and Bruggermann models, whereas the metal particles were modeled as ellipsoids of uniform size. The calculations gave the enhancement of the absorption within 15–150 depending upon the particle shape and the degree of interaction between the particles.[64,65]

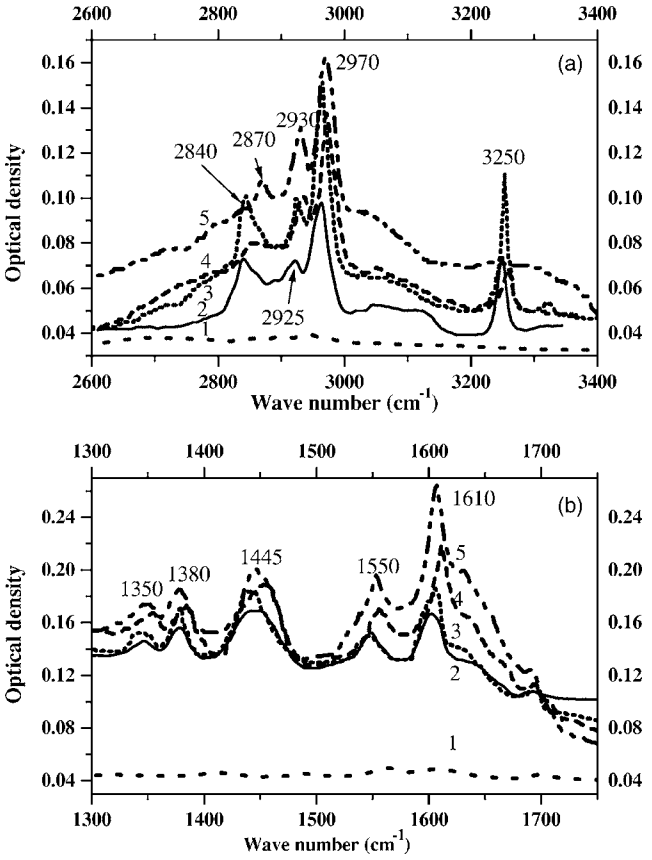

FIG. 7. Optical-density spectra for 1 μm thick AgI film (1) after dark adsorption of DEA molecules for 10 h at a 10 mbar pressure (dotted line) and [(2)–(5)] after illumination in DEA vapor for (illumination time t), (2) $t=10$ min (solid line), (3) $t=30$ min (short-dotted line), (4) $t=1$ h (short-dashed line), and (5) $t=10$ h (short-dotted-dashed line).

Except for "the electric-field enhancement," the other type of the enhancement was assumed, namely, "chemical enhancement," which provides an increase of $\delta\mu/\delta Q$ due to chemical interaction between the adsorbed molecule and the metal surface.[65] The total enhancement achieved by SEIRA is not as great as for SERS in the visible range, but still the enhancement factor of 1000 can be reached.[64]

The optical-density spectra of the AgI films evaporated onto IR-transparent KBr substrates were measured after various exposures. The double-beam spectrometer Specord-75 IR (Carl Zeiss) was used for this purpose.

Figure 6 presents the optical-density spectra for DEA vapor and liquid measured in a closed cell with KBr windows, whereas Fig. 7 those registered before and after several exposures of the AgI films in DEA vapor. The absorption bands shown in Figs. 6 and 7 can be divided into two groups: the bands in the range 2000–4000 cm^{-1} attributed to the C–H stretching vibrations in CH_2 and CH_3 groups and the N–H stretching vibrations in DEA molecules [Figs. 6(a) and 7(a)], and the bands in the range 1200–2000 cm^{-1} attributed to the stretching vibrations of C–N and C–C bonds and the bending vibrations of -CH_2, -CH_3, and N–H groups [Figs. 6(b) and 7(b)].

It is easy to identify the bands connected with the C–H stretching vibrations in CH_2 and CH_3 groups in the range 2700–3000 cm^{-1}, whereas the bending vibration of these groups are revealed at $\nu=1380$ cm^{-1} and $\nu=1450$ cm^{-1}. [58] The positions of the bands attributed to vibrations within these groups do not differ much in vapor and liquid (Fig. 6). The band connected with the N–H stretching vibration behaves differently: being barely observed at $\nu=3360$ cm^{-1} in vapor [Fig. 6(a), curve 1], it turns into a doubly peaked at $\nu=3290$ cm^{-1} and $\nu=3380$ cm^{-1} wide intensive band in liquid due to the formation of an association of DEA molecules [Fig. 6(a), curve 2]. The Fermi resonance seems to appear the most probable reason for the band splitting. A new band peaked at $\nu=1650$ cm^{-1} attributed to the N–H bending vibrations[58] also appears in liquid, whereas it is barely observed in vapor.

Before illumination, the adsorption of the hydrogen donors was provided by dark storage of the films in the closed cell for 10 h at a 10 mbar pressure of DEA. The optical-density spectrum measured after this process is presented in Fig. 7, curve 1. One can only observe very weak and barely seen absorption bands at $\nu=2970$, 1550, and 1610 cm^{-1}.

After illumination in DEA vapor, the intensity of the bands attributed to the vibrations within the adsorbed molecules is drastically enhanced. The narrow band attributed to the N–H stretching vibrations appears at $\nu=3250$ cm^{-1} (Fig. 7, curve 2). The great shift of the band position, as compared with that in liquid, indicates the N–H bond lengthening due to perturbation of this bond, which confirms that adsorbed DEA molecules are coordinated to surface Ag^+ cations via nitrogen atoms. The significant band narrowing, as compared with that in liquid, is attributed to the fact that SEIRA concerns the adsorbed molecules only in the nearest vicinity to the metal particle. The band at $\nu=3250$ cm^{-1} being slightly enhanced at the early stage of the illumination [Fig. 7(a), curve 3] decreases noticeably after long exposures (curve 4), vanishing finally at the end of the illumination (curve 5). The total disappearance of the band attributed to the N–H stretching vibration in DEA molecule indicates the N–H bond rupture, with hydrogen atoms which yield the hydrogen photosensitization of the halide being detached predominantly from these bonds. The band peaked at $\nu=2840$ cm^{-1} and attributed to the stretching vibrations of CH_2 and CH_3 groups in DEA molecule[57,66] exhibits similar behavior during illumination. First, it is slightly enhanced (curve 3), and then it starts to degenerate (curve 4), disappearing totally at the end of the illumination (curve 4); a new band peaked at $\nu=2870$ cm^{-1} (curve 5) appears in the spectrum. The band attributed to the N–H bending vibration in DEA molecule is not revealed in the AgI film spectra, perhaps due to its masking by the intensive band at $\nu\approx1610$ cm^{-1}. The bands at $\nu=1380$ cm^{-1} and $\nu=1450$ cm^{-1} do not undergo significant changes during illumination.

On the other hand, the appearance and the continuous growth of new wide bands peaked at about $\nu\approx2900$ cm^{-1} and $\nu\approx3300$ cm^{-1} can be observed, which may occur due to the formation of O–H bonds as the result of the reaction between detached hydrogen atoms and adsorbed ambient oxygen atoms. The other reason may be the formation of hydrogen bonds between the detached hydrogen atoms and surface iodine atoms of the halide film.

The bands at $\nu=1350$, 1550, and 1610 cm^{-1} may be assigned to the products of decomposition of the adsorbed mol-

ecules as the result of the reaction with adsorbed ambient oxygen or water. The doublet at $\nu=1350$ and 1550 cm^{-1} is typical for symmetric and antisymmetric stretching vibrations of surface COO^- groups, whereas the band at $\nu=1610$ cm^{-1} is a sign of the C=O stretching vibration of a carbonyl group.[66,67] The appearance of the carbonyl structures on the halide surface indicates that hydrogen atoms are photodetached also from the CH groups. At the initial stage of the illumination, the enhancement of the bands attributed to the vibrations within DEA molecules can occur due to a rapid increase of the concentration of the molecules adsorbed in the nearest vicinity to the photolytic silver particles; at longer exposures, this increase is counteracted by the detachment of hydrogen atoms from DEA molecules, the formation of radicals, and the oxidation of a part of the newly formed radicals to volatile products.

All these changes are observed due to the SEIRA. It is possible to make very rough estimations of the enhancement reached due to the SEIRA. Using formula (6), we can estimate an apparent molar extinction coefficient ε_a for the IR absorption bands as follows:

$$\varepsilon_a = D/dc. \tag{12}$$

For example, the value of the photoinduced optical density for the band attributed to the N–H stretching vibration taken after subtraction of the background absorption is 0.06 (Fig. 7, curve 1), with film thickness $d=10^{-4}$ cm; as before, the concentration of DEA molecules is assumed to be ~0.1–0.5 mol/l. Then, one gets $\varepsilon_a \approx (1.15-5.76)\times 10^3$ l/mol cm. Reference[57] gives the value for the bands connected with the N–H stretching vibrations as $\varepsilon_a \sim 20$ l/mol cm for free molecules. It means that surface enhancement of the IR absorption band attributed to the N–H stretching vibration is within 60–300.

The other estimation can be made by comparison of the absorption integrals for the bands which can be registered after the dark absorption of DEA molecules and after illumination. For example, the enhancement calculated as the ratio of the areas under the absorption curves for the band at $\nu=2870$ cm^{-1} before and after the first exposure gives ~60. One could assume this value as the lowest limit for the enhancement: in the absence of the silver colloids, one measures the absorption of the total number of the adsorbed molecules, whereas only a part of them in the close vicinity to the arising silver particles acquire the enhancement in the absorption band intensity. At the same time, one would expect the difference in the enhancement for various absorption bands. For example, the absorption due to the N–H stretching vibration is expected to have higher enhancement since the adsorbed molecule is coordinated to the halide surface via nitrogen atom. Averaging, the enhancement of ~100 as the order of the magnitude can be assumed. Meanwhile, the theory gives for SEIRA the possible value of the enhancement up to 1000.[64,65]

It has bean shown that several kinds of silver particles arise under illumination in the AgI films; the next task to be discussed is which ones are responsible for the SEIRA. The magic clusters may be excluded from this consideration since they are not metallic and have very small size. One should choose between two types of metallic silver colloids: the small-sized particles and the large-sized particle with complicated morphology. For this reason, an attempt was made to observe the SEIRA in the $RbAg_4I_5$ films under the same conditions as for the AgI films. The printout effect carried out in the $RbAg_4I_5$ films yielded much attenuated SEIRA as compared with that in the AgI films, which, in turn, makes it possible to conclude unambiguously that the SEIRA is attributed to the small-sized (<20 nm) metallic colloids, which ensure the largest surface for the adsorption of the organic molecules. As it was discussed before, much bigger concentration of the small-sized particles was achieved in the AgI films by the photolysis as compared with the $RbAg_4I_5$ films. It is clear that the AgI films are the best candidates for being the substrate for SEIRA among the silver halide films. Currently proceeding experiments with atomic force microscopy and Raman can forward further elucidation of this process.

V. CONCLUSIONS

Two methods of the hydrogen photosensitization of AgI films were invented. The direct photoinjection of hydrogen carried out in the AgI polycrystalline films via the photoinitiated hydrogen transfer provides the sensitization centers for deeper photolysis of AgI as compared with the hydrogen spillover, which makes it possible to distinguish various stages of the photochromism and to elucidate its mechanism. Being an excellent reducing agent, atomic photochemical hydrogen provides hydrogen doping and hydrogen sensitization, whose main spirit is that it is achieved under the action of the same source of light. The sensitization, in turn, triggers the photolysis. The other spirits are the fracture of grains, the appearance of nanosized "magic" silver clusters and nanosized metal silver colloids during the photolysis, which yields SEIRA.

The photolytic metallic silver colloids of size <20 nm serve as substrates for SEIRA for hydrogen-donor molecules. The AgI films seem to be the best candidate for being the substrate for SEIRA, due to the highest inclination to form the small-sized silver colloids as compared with the other silver halides. This process may be of great interest for engineering of photonic crystals and for other phototechnologies, as well as for catalysis on nanosized particles. In fact, a composite material possessing interesting properties was created, consisting of the AgI particles, the Ag particles of various sizes, the adsorbed DEA molecules, and the products of their decomposition.

This work underlines the exclusive importance of the surface morphology for the silver halides, recognized photographic materials. Grain size and shape, surface roughness, size and shape of pores, inner cavities, and grain interlayer boundaries determine the character of adsorption of hydrogen-containing species. The experiments presented show that the great difference in the photosensitivity, which the AgI "nonsensitized" films demonstrate in comparison with the nonsensitized AgCl, or the $RbAg_4I_5$ evaporated films, depends rather upon the specific surface area and surface morphology than upon internal parameters. Under nor-

mal conditions, the evaporated nonsensitized AgCl, or the $RbAg_4I_5$ films, which have much larger specific surface area and roughness as compared with that in the AgI films, can undergo the uncontrolled hydrogen sensitization due to adsorption of various hydrogen-containing molecules and following surface reactions which yield hydrogen atoms necessary for creation of the sensitization centers. The paper presented manifests the exclusive importance of investigations of the behavior of hydrogen, which is very often a latent catalyst for many surface processes.

The paper presents the whole batch of the novel effects which are connected with hydrogen. The process starts from a hydrogen abstraction reaction producing photochemical hydrogen which, in turn, is used to provide hydrogen excitation (sometimes via hydrogen spillover) of the halide surface. The hydrogen excitation leads to the hydrogen sensitization simultaneous to illumination, the photolysis of the AgI films, and the growth of nanosized silver colloids and clusters, which, in turn, can be used as catalysts for hydrogen production. On the other hand, the silver particles are good substrates for observing SEIRA, which is achieved by adsorption of the hydrogen-donor molecules. SEIRA, in turn, serves as an instrument for the investigation of the hydrogen abstraction reaction which had initiated the whole process; one can observe a very interesting cycle of events.

It should also be mentioned that the hydrogen abstraction reaction is the very first stage of photosynthesis, and this is the main reason stimulating the interest to these reactions. The paper presented shows that there is an intriguing connection between photosynthesis and photography and hydrogen is a point which can connect these famous subjects.

Further intensive investigations are needed to elucidate all details of these interesting phenomena.

[1] S. Hull, Rep. Prog. Phys. **67**, 1233 (2004).
[2] P. J. Demott, Atmos. Res. **38**, 63 (1995).
[3] X. Guo, G. Zheng, and D. Jin, Atmos. Res. **79**, 183 (2006).
[4] T. H. James, in *The Theory of the Photographic Process*, edited by T. H. James (Macmillan, New York, 1966), p. 165.
[5] N. F. Mott and R. W. Gurney, *Electronic Processes in Ionic Crystals* (Clarendon, Oxford, 948).
[6] H. Ogura and T. Ogura, J. Imaging Sci. Technol. **38**, 222 (1994).
[7] J. Belloni, Radiat. Phys. Chem. **67**, 291 (2003).
[8] W. C. Bell and M. L. Myrick, J. Colloid Interface Sci. **242**, 300 (2001).
[9] J. Belloni, M. Mostafavi, H. Remita, J. L. Marignier, and M. O. Delcourt, New J. Chem. **22**, 1239 (1998).
[10] R. He, X. Qian, J. Yin, and Z. Zhu, J. Mater. Chem. **12**, 3783 (2002).
[11] Y. Sun and Y. Xia, Analyst (Cambridge, U.K.) **128**, 686 (2003).
[12] P. Mulvaney, Langmuir **12**, 788 (1996).
[13] K. Patel, S. Kapoor, D. Dave, and T. Mukherjee, J. Chem. Sci. **117**, 53 (2005).
[14] M. H. G. Miranda, E. L. Falcão-Filho, J. J. Rodrigues, Jr., Cid B. de Araújo, and L. H. Acioli, Phys. Rev. B **70**, 161401(R) (2004).
[15] J. Widoniak, S. Eiden-Assmann, and G. Maret, Colloids Surf., A **270-271**, 340 (2005).
[16] U. Kreibig, M. Quinten, and D. Schoenauer, Physica A **157**, 244 (1986).
[17] R. He, X. Qian, J. Yin, and Z. Zhu, J. Mater. Chem. **12**, 3783 (2002).
[18] A. Henglein, J. Phys. Chem. **97**, 5457 (1993).
[19] A. Henglein, Chem. Mater. **10**, 444 (1998).
[20] C. Xia and Y. Sun, Science **298**, 2176 (2002).
[21] C. Xia and Y. Sun, Adv. Mater. (Weinheim, Ger.) **15**, 695 (2003).
[22] S. M. Heard, F. Grieser, and C. G. Barraclough, J. Colloid Interface Sci. **93**, 545 (1983).
[23] N. Satoh, H. Hasegawa, K. Tsuji, and K. Kimura, J. Phys. Chem. **98**, 2143 (1994).
[24] J. Zhang, X. Li, K. Liu, Z. Cui, G. Zhang, B. Zhao, and B. Yang, J. Colloid Interface Sci. **55**, 115 (2002).
[25] X. Li, W. Xu, J. Zhang, H. Jia, B. Yang, B. Zhao, B. Li, and Y. Ozaki, Langmuir **29**, 1298 (2004).
[26] S. Zhao, K. Zhang, J. An, Y. Sun, and C. Sun, Mater. Lett. **60**, 1215 (2006).
[27] H. Jia, J. Zeng, W. Song, J. An, and B. Zhao, Thin Solid Films **496**, 281 (2006).
[28] A. Gavrilyuk, Proc. SPIE **2968**, 213 (1997).
[29] A. I. Gavrilyuk, Tech. Phys. Lett. **19**, 703 (1993) [Pis'ma Zh. Tekh. Fiz. **19**, 1 (1993)].
[30] A. I. Gavrilyuk, Tech. Phys. Lett. **19**, 718 (1993) [Pis'ma Zh. Tekh. Fiz. **19**, 44 (1993)].
[31] A. I. Gavrilyuk and T. G. Lanskaya, Thin Solid Films **515**, 2337 (2006).
[32] J. F. Gamilton, Adv. Phys. **37**, 359 (1988).
[33] K. Matsunaga, I. Tanaka, and H. Adachi, J. Phys. Soc. Jpn. **67**, 2027 (1998).
[34] A. A. Barmasov, L. K. Kudrjashova, V. A. Resnikov, and A. L. Kartuzhansky, Pis'ma Zh. Tekh. Fiz. **15**, 83 (1990).
[35] T. E. Kehva, A. L. Kartuzhansky, and V. A. Resnikov, Zh. Fiz. Khim. **65**, 1485 (1991).
[36] R. Ostwald and K. G. Weil, J. Vac. Sci. Technol. **6**, 684 (1969).
[37] T. Tani, J. Imaging Sci. Technol. **48**, 278 (2004).
[38] W. G. Lowe, J. E. Jones, and H. E. Roberts, in *Fundamentals of Photographic Sensitivity*, Proceedings of Bristol Symposium 1950, edited by J. W. Mitchell (Butterworth Science, London, 1951), p. 112.
[39] T. Tani, J. Imaging Sci. Technol. **41**, 577 (1997).
[40] S. K. Deb, Philos. Mag. **27**, 801 (1973).
[41] C. G. Granqvist, *Handbook of Inorganic Electrochromic Materials* (Elsevier, Amsterdam, 1995).
[42] T. He and J. N. Yao, Prog. Mater. Sci. **51**, 810 (2006).
[43] T. He and J. N. Yao, Res. Chem. Intermed. **30**, 459 (2004).
[44] A. I. Gavrilyuk, Ionics **4**, 372 (1998).
[45] A. I. Gavrilyuk, Electrochim. Acta **44**, 3027 (1999).
[46] A. I. Gavrilyuk, in Proceedings of the 2001 International Semiconductor Device Research Symposium, Washington, 5–7 December 2001 (unpublished), p. 55.
[47] A. I. Gavrilyuk, U. Tritthart, and W. Gey, Philos. Mag. Lett. **86**, 205 (2006).

[48] A. I. Gavrilyuk, T. G. Lanskaya, A. A. Mansurov, and F. A. Chudnovskii, Sov. Phys. Solid State **26**, 117 (1984) [Fiz. Tverd. Tela (Leningrad) **26**, 200 (1984)].
[49] A. I. Gavrilyuk, T. G. Lanskaya, and F. A. Chudnovskii, Sov. Phys. Tech. Phys. **32**, 964 (1987) [Zh. Tekh. Fiz. **57**, 1617 (1987)].
[50] C. B. Lutschik, I. K. Vitol, and M. A. Elango, Usp. Fiz. Nauk **122**, 223 (1977).
[51] M. I. Klinger, C. B. Lutschik, T. V. Mashovetz, G. A. Holodar, M. K. Sheinkman, and M. A. Elango, Usp. Fiz. Nauk **147**, 523 (1985).
[52] M. Cardona, Phys. Rev. **129**, 69 (1963).
[53] A. L. Despotuli, in *New Trends in International Compounds for Energy Storage*, edited by C. Julien, J. P. Ramos-Pereira, and A. Momchilov, NATO Science Series II: Mathematic Physics, and Chemistry (Springer, New York, 2002), Vol. 61, p. 455.
[54] A. L. Despotuli, V. I. Levashov, and L. A. Matveeva, Russ. J. Electrochem. **39**, 472 (2003).
[55] *Physics of II-VI and I-VI Compounds: Semimagnetic Semiconductors*, Landolt-Börnstein, New Series, Group III, Vol. 17, Pt. B (Springer-Verlag, Berlin, 1982), p. 496.
[56] R. Cukier and D. Nocera, Annu. Rev. Phys. Chem. **49**, 337 (1998).
[57] J. C. D. Brand and G. Eglinton, *Applications of Spectroscopy to Organic Chemistry* (Oldbourne, London, 1965).
[58] B. G. Ershov, Izv. Ross. Acad. Nauk, Ser. Khim. **1**, 1 (1999).
[59] R. K. Chang and T. E. Furtak, *Surface Enhanced Raman Scattering* (Plenum, New York, 1982).
[60] H. Metiu, Prog. Surf. Sci. **17**, 153 (1984).
[61] M. Moskovits, Rev. Mod. Phys. **57**, 783 (1985).
[62] A. Otto, I. Mrozeck, H. Grabhorn, and W. Akemann, J. Phys.: Condens. Matter **4**, 1143 (1992).
[63] W. B. Fisher, G. Steiner, C. Kuhne, and R. Salzer, J. Mol. Struct. **570**, 153 (2001).
[64] M. Osawa, Top. Appl. Phys. **81**, 185 (2001).
[65] M. Osawa, K. Ataka, K. Yoshi, and Y. Nishikawa, Appl. Spectrosc. **47**, 1497 (1993).
[66] R. L. Loriner, R. S. Fuson, D. Y. Curtin, and T. C. Morril, *The Systematic Identification of Organic Compounds* (Wiley, New York, 1980).
[67] A. A. Davydov, *IR-Spectroscopy in Chemistry of the Oxide Surface* (Nauka, Novosibirsk, 1984).